Eleventh International Conference on CFD in the Minerals and Process Industries
CSIRO, Melbourne, Australia
7-9 December 2015

INVESTIGATING STOMACH MIXING AND EMPTYING FOR AQUEOUS LIQUID CONTENTS USING A COUPLED BIOMECHANICAL-SMOOTHED PARTICLE HYDRODYNAMICS MODEL

Simon M. HARRISON[1,2*], Paul W. CLEARY[1,2] and Matthew D. SINNOTT[1,2]

[1]CSIRO Data61, Clayton, Victoria 3169, AUSTRALIA
[2]CSIRO Food and Nutrition, Clayton, Victoria 3169, AUSTRALIA
*Corresponding author, E-mail address: Simon.Harrison@csiro.au

ABSTRACT

The stomach is a critical organ for food digestion but it is not well understood how the stomach operates, either when it is healthy or when dysfunction occurs. Stomach function depends on the timing and amplitude of stomach contractions, the fill level of contents and the type of gastric contents. Using a coupled biomechanical-Smoothed Particle Hydrodynamics (B-SPH) model, we investigate how gastric discharge is affected by the contraction behaviour of stomach wall and the viscosity of the contents. The results of the model provide new insights into how the content viscosity and the number of compression waves down the length of the stomach affect the flow rate of the contents exiting the stomach to the duodenum. This investigation evaluates the ability of a B-SPH model for simulating complicated stomach behaviour. Gastric emptying is found to increase with a greater number of contractile waves and strongly decrease with increasing gastric content viscosity. Future studies will determine how anatomical movements and stomach contents affect the residence time of food in the stomach.

INTRODUCTION

The stomach is an important organ that mixes and comminutes the products of ingestion and mastication and provides control of nutrient and drug delivery to the intestines and circulatory system. Stomach function has typically been studied using limited *in vivo* measurements (Ajaj et al., 2004; Rao et al., 1996) or *in vitro* experiments (Guerra et al., 2012; Kong and Singh, 2010) but the mixing and emptying behaviour cannot be fully characterised by these methods. Computational simulation has the capacity to provide understanding where measurements are not practical or ethically allowed. Currently, studies have focused on how the stomach mixes purely liquid contents (Pal et al., 2004, 2007; Ferrua and Singh, 2010; Kozu et al., 2010; Xue et al., 2012; Du et al., 2013; Imai et al., 2013; Cleary et al., 2015) and only one study has considered how these contents are emptied into the intestines (Pal et al., 2007).

After mastication in the mouth, food enters the stomach from the oesophagus and is churned by contractions of the stomach wall. Acids and other digestive chemicals are secreted and mixed with the food bolus to accelerate the digestive process. After a suitable amount of breakdown the food fragments are emptied through the pyloric sphincter into the small intestine where further breakdown and nutrient uptake occurs. Stomach function depends on the timing and amplitude of stomach contractions, the fill level of contents and the load of solid contents. It is not well understood how the stomach operates, either when it is healthy or when dysfunction occurs.

Emptying is thought to be controlled by restriction of the pyloric sphincter and contractions in the duodenum, which are induced by exposure of the duodenum to acid or lipids (Rao et al., 1996). Aqueous (non-lipid containing) stomach contents can pass through the stomach without measureable restriction from the muscles distal to the stomach, including the pyloric sphincter (Tougas et al., 1992). However, when substantial oil (lipid) contents are detected by the duodenum, the pyloric sphincter closes and retention time of gastric contents is much longer (Tougas et al., 1992).

Using a B-SPH model, we investigate stomach emptying for non-lipid containing liquids, where the pyloric sphincter is consistently fully open. Changes to gastric flow due to changes in the contraction behaviour of stomach wall and the viscosity of the contents are investigated. The model comprises a biomechanical model of the stomach wall and an SPH representation of aqueous stomach contents. The large antral contraction waves (ACWs) that travel down the stomach wall are prescribed in the model as rigid deformations of the stomach wall. Using this model, we investigate the emptying behaviour of the stomach and the sensitivity of model results to input parameters.

COMPUTATIONAL MODEL

Smoothed Particle Hydrodynamics

SPH is a mesh-free Lagrangian particle method for solving partial differential equations. Fluid dynamics applications of the method are detailed in Monaghan (1994, 2005) and Cleary et al. (2007). Volumes of fluid are represented by a moving set of particles, over which the Navier Stokes equations can be reduced to the following ordinary differential equations:

$$\frac{d\rho_a}{dt} = \sum_b m_b \mathbf{v}_{ab} \cdot \nabla_a W_{ab} \tag{1}$$

$$\frac{d\mathbf{v}_a}{dt} = -\sum_b m_b \left[\left(\frac{P_b}{\rho_a^2} + \frac{P_a}{\rho_a^2} \right) - \frac{\xi}{\rho_a \rho_b} \frac{4\mu_a \mu_b}{(\mu_a + \mu_b)} \frac{\mathbf{v}_{ab} \cdot \mathbf{r}_{ab}}{\mathbf{r}_{ab}^2 + \eta^2} \right] + \mathbf{g} \tag{2}$$

where ρ_a is the density of particle a, t is time, m_b is the mass of particle b and $\mathbf{v}_{ab} = \mathbf{v}_a - \mathbf{v}_b$, where $\mathbf{v}_a$ and $\mathbf{v}_b$ are the velocities of particles a and b. W is a cubic-spline interpolation kernel function that is evaluated for the

distance between particles a and b. P_a and μ_a are the local pressure and dynamic viscosity for particle a, η is a small number to mitigate singularities when the denominator is small, ξ is a normalisation constant for the kernel function and **g** is the gravitational acceleration.

A quasi-compressible formulation of the SPH method is employed. The equation of state for such a weakly compressible fluid relates the fluid pressure, P to the particle density, ρ:

$$P = \frac{c^2 \rho_0}{\gamma}\left[\left(\frac{\rho}{\rho_0}\right)^{\gamma} - 1\right] \tag{3}$$

where c is sound speed and the reference density is given by ρ_0. γ is a material constant, which is equal to 7 for fluids with properties similar to water. A mach number of approximately 0.1 is used to reduce density variations from compressibility effects to the order of 1%.

A second order predictor-corrector integration scheme given in Monaghan (1994) is used. The time step is chosen so that it satisfies the Courant condition with a modification for the presence of viscosity (see Cleary, 1998):

$$\delta t = \min_a \left(0.5 \cdot h \Big/ \left(c + \frac{2\xi\mu_a}{h\rho_a} \right) \right) \tag{4}$$

This formula guarantees stability of the numerical integration

Nodes of boundary objects are represented as boundary SPH particles, which are repositioned at every time step as a result of both rigid body motion and/or deformation of the boundary. The wall of the stomach (described below) is deformed by antral contraction waves (ACWs) propagating down towards the pyloric sphincter.

SPH model of the stomach contents

The stomach was filled to 80% with an initially stationary Newtonian fluid of a constant viscosity. Stomach contents can vary from water with a viscosity of 0.001 Pa s to a thick slurry with a viscosity of 1 Pa s (Ferrua and Singh 2010). The effect of viscosity on mixing and emptying was investigated using four values that span the representative range: 0.01 Pa.s, 0.03 Pa.s, 0.1 Pa.s and 1.0 Pa.s in separate simulations. Back pressure on the fluid leaving the stomach, due to downstream intestinal contractions is modelled using a constant pressure outflow boundary condition after the pyloric sphincter. The back pressure is assumed to be 400 Pa, which is approximately 50% of the hydrostatic pressure at the pyloric sphincter (using an 86 mm initial depth of fluid). This is similar in magnitude to manometry readings for the pyloric region of the stomach (Tougas et al., 1992) during emptying. The sensitivity of model results to the choice of back pressure is investigated using two pressure levels (400 Pa and 500 Pa) in separate simulations.

Biomechanical model of the contracting stomach

Figure 1 shows a schematic of the stomach model. The stomach wall is represented in the computational model by a deforming surface mesh. The mesh comprises 15,000 nodes, spaced at an average separation of 3 mm. The deformation of the surface mesh is a kinematically prescribed input according to measurements by Ferrua and Singh (2010). The mesh is rigged to a set of rings, which reduce in radius according to the speed and occlusion of each ACW.

Figure 2 shows the deformation of the stomach model for a simulation case with three simultaneous ACWs. Each ACW travels down the stomach at a speed of 2.2 mm/s along the centreline (Ferrua and Singh, 2010). With a centreline length of 13.3 cm, the ACW duration is 60 s. The effect of varying the number of ACWs was investigated by considering three different inter-wave periods: 20 s (giving 3 simultaneous waves at different locations in the stomach), 40 s (2 simultaneous waves) and 60 s (one wave at a time).

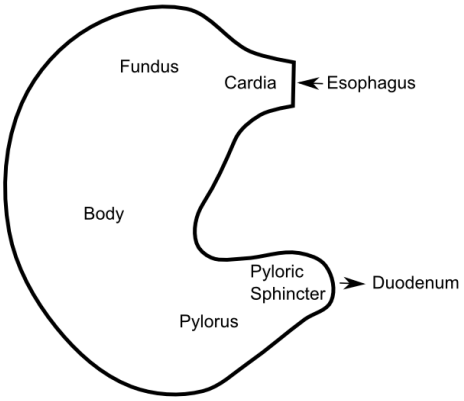

Figure 1: The anatomical model of the stomach which is a hollow digestive organ. The food bolus enters from the oesophagus at the cardia. The superior section is the fundus and is often not filled with liquid/solids; the middle section is the body (or corpus); and the inferior section is the pylorus. Once mixing and digestion have occurred the contents leave the stomach through the pyloric sphincter into the duodenum, which leads to the small intestine.

RESULTS AND DISCUSSION

Figure 3 shows the mixing flow of fluid in a central cross-sectional plane through the stomach during discharge for inter-ACW periods of 20 s, 40 s and 60 s. The contraction waves start at the top and propagate downwards. In regions of high contraction, the fluid is forced to move quickly away from the converging stomach surfaces. At 30 s (Figure 3a) the peak contraction is about 2/3 of the way down the stomach. Fluid is fairly quiescent above this but flows quickly within and away from the constricted area. The contractile state of the stomach is the same for each of the three wave periods (shown in Figure 3 as columns) at this time so the flow is very similar for the three cases. At 60 s (Figure 3b) the stomach contraction has dissipated for the period=60 s case (left) and so the fluid velocities have substantially slowed. Higher speed flow is only observed near the pyloric sphincter. In contrast, the contraction in the period=40 s case (middle column) has reasonable flow speeds throughout much of the content. For the period=20 s case (right column) the contraction has almost reached the lower end of the stomach and flow speeds are high throughout. The free surface level declines through each simulation due to the discharge generated by the contraction of the stomach. The amount of emptying visibly increases with the decrease in contraction period (since there is more contractile activity driving the flow). At 90 s, (Figure 3c) the second wave for the period=60 s case is now in the same location as for the first wave (Figure 3a) and generates similar intensity flow but with a lower free surface due to the discharge. The period=20 s case shows the contractile wave just arriving at the location of the pyloric sphincter and there is a strong and coherent flow out through the end of the stomach into the small intestine. Figures 3d and e show the state of the stomach and contents for another half and one full contraction cycle for the period=60 s case.

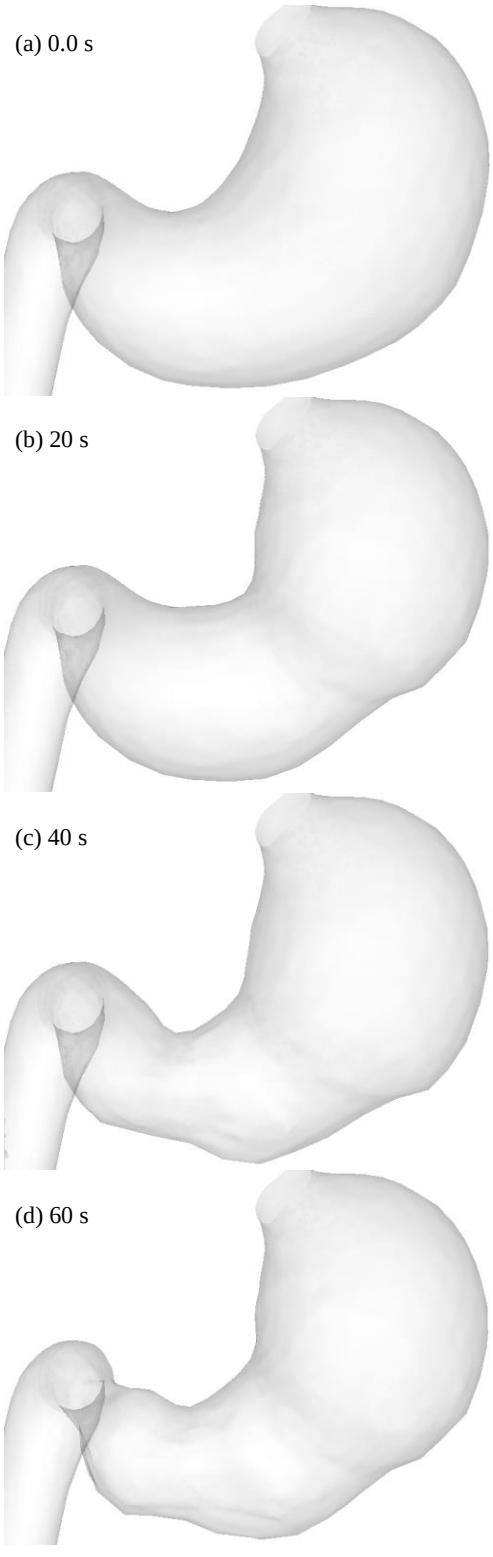

Figure 2: Model representation of antral contractile waves (ACWs) moving down the stomach towards the pyloric sphincter. The wave occurs every 20 s (resulting in three waves being present at different locations in the stomach at any point in time). These are inputs into the model.

The multiple overlapping contractile waves (period=20 s case) are very effective at creating discharge flow and lowering the level of fluid content in the stomach. As a general observation, high fluid speeds occur below the regions of peak contraction of the stomach wall and this flow is a combination of discharge flow out of the stomach and vortex induced mixing within the stomach contents.

Figure 4 shows the mass flow rate through the pyloric sphincter for inter-ACW periods of 20 s, 40 s and 60 s for a viscosity of 0.01 Pa.s. In all cases there are high frequency fluctuations driven by the details of the fluid flow in the lower stomach which are not important. The underlying flow rate for the period=20 s case (with 3 simultaneous waves) declines linearly with time due to the decreasing pressure head as the stomach content empties. However as the inter-ACW period increases and the number of simultaneous waves decreases then long period coherent cyclic variations are observed in the flow rate. For an inter-ACW period of 40 s (2 simultaneous waves) the mass flow rate has minima corresponding to the start of each wave (at 40 s, 80 s etc). For an inter-ACW period of 60 s (1 wave at a time) the mass flow rate reduces substantially after the first 20 s of wave transit. The flow speeds inside the stomach content decline and the fluid becomes substantially quiescent. It would appear that overlapping of the ACWs is able to eliminate the long period cyclic behaviour and produce a nearly linear discharge rate. The average discharge rate from the stomach (given in Table 1) decreases steadily with increasing inter-ACW period. Since this period is often observed to be around 20 s (Ferrua and Singh, 2010), it is possible that this wave frequency is in a sense optimal for steady emptying of the stomach.

Figure 5 shows the mixing and discharge of fluid in a central cross-section of the stomach for viscosities of low (0.01 Pa.s) and high (1.0 Pa.s) viscosities. Flow speeds are significantly reduced by stronger viscous forces with the mixing flow in the main volume of the stomach particularly strongly affected. Discharge flow through the pyloric sphincter is still observed but it is much gentler.

Figure 6 shows the mass flow rate through the pyloric sphincter for viscosities of 0.01 Pa.s, 0.03 Pa.s, 0.1 Pa.s and 1.0 Pa.s. The rate is strongly proportional to viscosity. The pattern of time variation is similar for the different viscosities. The average mass flow rate for the different viscosities is shown in Table 2 and shows that the discharge rate increases logarithmically with decreasing viscosity.

Finally, Figure 7 shows the mass flow rate through the pyloric sphincter for duodenal back pressures of 400 and 500 Pa. There are only very small differences in the short time scale fluctuations with the underlying mass flow rate being insensitive to viscosity and both the magnitude and the long term variation being the same for the two pressures. The average mass flow rates are given in Table 3 and show that there is little change with the fluid back pressure. This shows that the discharge dynamics are entirely controlled by the pressures and flow generated within the stomach as a result of the nature of the contraction behaviour, the fill level and the fluid viscosity.

Future work will focus on model verification and validation. Sensitivity of results to model parameters such as particle size and stomach wall deformation specifications will be determined using a sensitivity study. Model outputs will be validated against measurements where available. Notably, the measurement of flow rates is difficult and needs to be done in tandem with characterisation of stomach contractile patterns to allow suitable comparison with the stomach model.

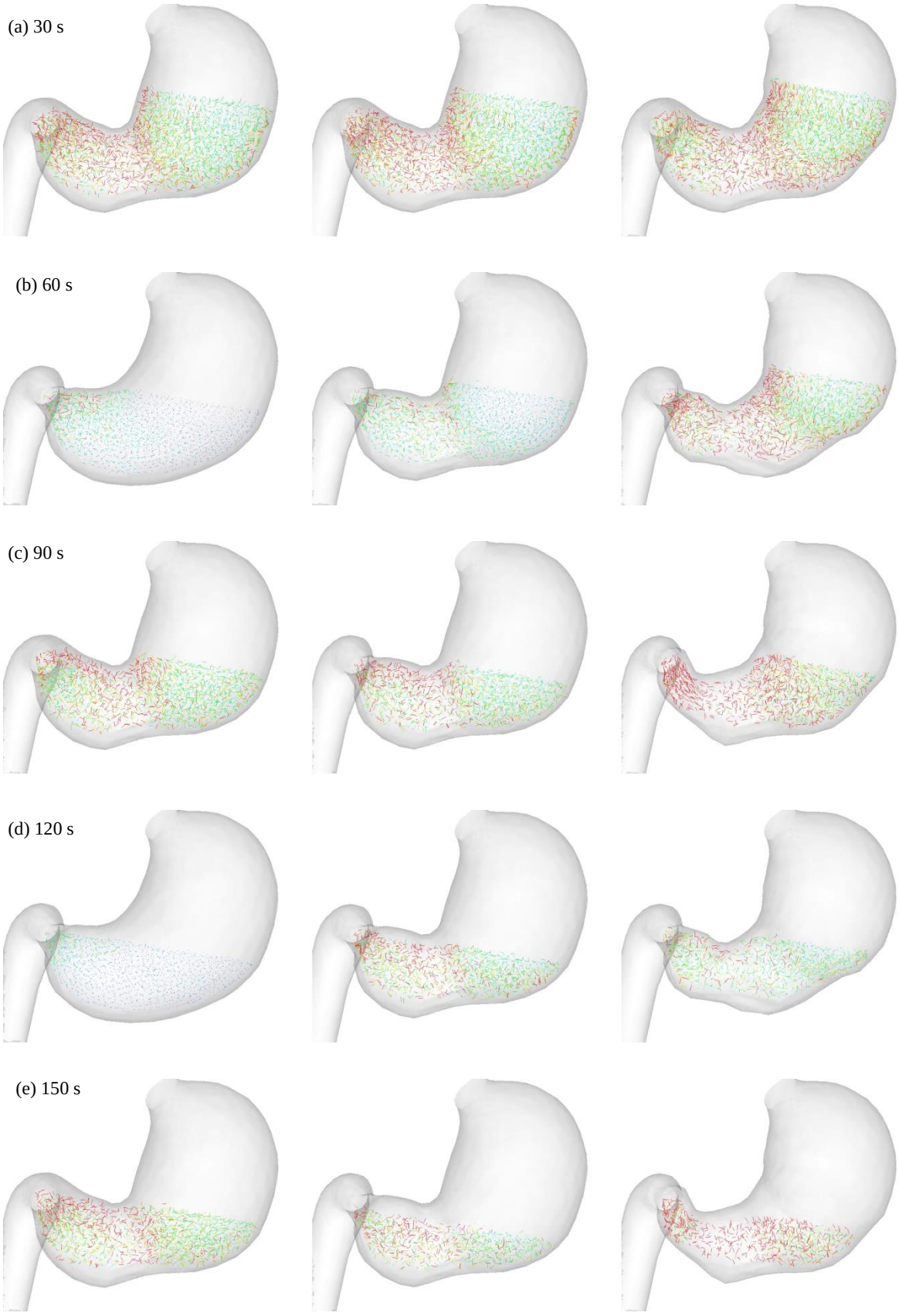

Figure 3: Fluid flow in a cross-sectional plane through the centre of the stomach showing progressive emptying. Flow velocities are represented by vectors with velocity dependent lengths and coloured by fluid speed (blue low, green intermediate and red is fast). The period between ACWs are: (left) period = 60 s; (middle) period = 40 s; and (right) period = 20 s.

This stomach model allows prediction of gastric mixing and emptying of the stomach for any prescribed contractile wave and content fill level and rheology. The presence of particulate solids and any non-Newtonian behaviour of the content will change these behaviours to some degree. This will be explored in future work.

Table 1: Mass flow rate through the pyloric sphincter for different inter-ACW periods.

Inter ACW period (s)	Mass flow rate (g / s)
20	82
40	72
60	53

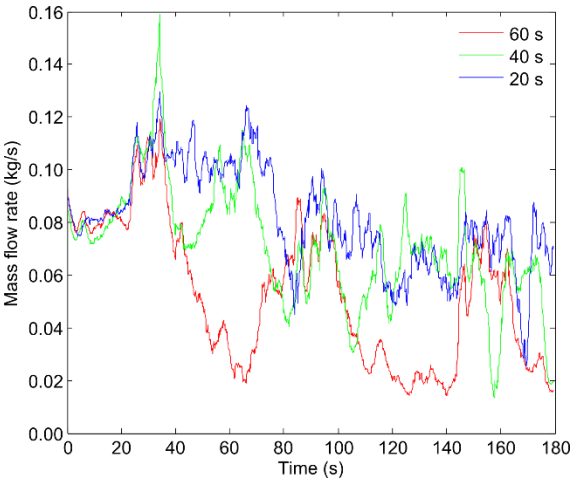

Figure 4: Mass flow rate through the pyloric sphincter for a viscosity of 0.01 Pa.s and inter-ACW periods of 20, 40, and 60 s.

Table 2: Variation of average mass flow rate through the pyloric sphincter with the viscosity of the gastric content.

Viscosity (Pa s)	Mass flow rate (g/s)
0.01	82
0.03	54
0.1	31
1.0	8.9

Table 3: Variation in the average mass flow rate through the pyloric sphincter for different back pressures.

Back pressure (Pa)	Mass flow rate (g/s)
400	82
500	81

CONCLUSION

A coupled B-SPH model of gastric emptying for non-lipid contents is presented. Using a detailed model of stomach contraction, simulations were performed of the mixing and discharge flow behaviour of gastric contents within the stomach and out through the pyloric sphincter. Shorter periods between antral contractile waves (AWCs) lead to higher and steadier discharge mass flow from the stomach. This occurs because the first 20 s of the wave propagation appears to contribute the most to generating the flow that leads to discharge. As the wave period increases the flow generated by each wave is able to substantively decline before the arrival of the next wave leading to a strong cyclic variation in the discharge rate. Gastric emptying was found to be strongly dependent on the viscosity but insensitive to back pressures in a sensible range of 400 to 500 Pa.

Future extensions of the model will include mixed solid and liquid contents and dynamic or static constrictions of the pyloric sphincter for mixing of lipid-containing contents.

REFERENCES

AJAJ, W., LAUENSTEIN, T., PAPANIKOLAOU, N., HOLTMANN, G., GOEHDE, S.C., RUEHM, S.G., DEBATIN, J.F., 2004. Real-time high-resolution MRI for the assessment of gastric motility: Pre- and post pharmacological stimuli. J. Magn. Reson. Imaging 19, 453–458. doi:10.1002/jmri.20029

CLEARY, P.W., 1998. Modelling confined multi-material heat and mass flows using SPH. Applied Mathematical Modelling 22, 981–993.

CLEARY, P.W., PRAKASH, M., HA, J., STOKES, N. and SCOTT, C. 2007. Smooth particle hydrodynamics: Status and future potential. Prog. Comput. Fluid Dyn. *7*, 70–90.

CLEARY, P.W., SINNOTT, M.D., HARI, B., BAKALIS, S., HARRISON, S.M., 2015. 10 - Modelling food digestion, in: Fryer, S.B.K.J. (Ed.), Modeling Food Processing Operations, Woodhead Publishing Series in Food Science, Technology and Nutrition. Woodhead Publishing, pp. 255–305.

DU, P., O'GRADY, G., GAO, J., SATHAR, S., CHENG, L.K., 2013. Toward the virtual stomach: progress in multiscale modeling of gastric electrophysiology and motility. Wiley Interdiscip. Rev. Syst. Biol. Med. 5, 481–493. doi:10.1002/wsbm.1218

FERRUA, M. J., SINGH, R. P., 2010. Modeling the Fluid Dynamics in a Human Stomach to Gain Insight of Food Digestion. J. Food Sci. 75, R151–R162. doi:10.1111/j.1750-3841.2010.01748.x

GUERRA, A., ETIENNE-MESMIN, L., LIVRELLI, V., DENIS, S., BLANQUET-DIOT, S., ALRIC, M., 2012. Relevance and challenges in modeling human gastric and small intestinal digestion. Trends Biotechnol. 30, 591–600. doi:10.1016/j.tibtech.2012.08.001

IMAI, Y., KOBAYASHI, I., ISHIDA, S., ISHIKAWA, T., BUIST, M., YAMAGUCHI, T., 2013. Antral recirculation in the stomach during gastric mixing. Am. J. Physiol. - Gastrointest. Liver Physiol. 304, G536–G542. doi:10.1152/ajpgi.00350.2012

KONG, F., SINGH, R.P., 2010. A Human Gastric Simulator (HGS) to Study Food Digestion in Human Stomach. J. Food Sci. 75, E627–E635. doi:10.1111/j.1750-3841.2010.01856.x

KOZU, H., KOBAYASHI, I., NAKAJIMA, M., UEMURA, K., SATO, S., ICHIKAWA, S., 2010. Analysis of Flow Phenomena in Gastric Contents Induced by Human Gastric Peristalsis Using CFD. Food Biophys. 5, 330–336. doi:10.1007/s11483-010-9183-y

MONAGHAN, J.J. 1994. Simulating free surface flows with SPH. J. Comput. Phys. *110*, 399–406.

MONAGHAN, J.J. 2000. SPH without a tensile instability. J. Comput. Phys. *159*, 290–311

PAL, A., BRASSEUR, J.G., ABRAHAMSSON, B., 2007. A stomach road or “Magenstrasse” for gastric emptying. J. Biomech. 40, 1202–1210. doi:10.1016/j.jbiomech.2006.06.006

PAL, A., INDIRESHKUMAR, K., SCHWIZER, W., ABRAHAMSSON, B., FRIED, M., BRASSEUR, J.G., 2004. Gastric flow and mixing studied using computer simulation. Proc. R. Soc. Lond. B Biol. Sci. 271, 2587–2594. doi:10.1098/rspb.2004.2886

RAO, S., LU, C., SCHULZE-DELRIEU, K., 1996. Duodenum as a immediate brake to gastric outflow: A videofluoroscopic and manometric assessment. Gastroenterology 110, 740–747. doi:10.1053/gast.1996.v110.pm8608883

TOUGAS, G., ANVARI, M., DENT, J., SOMERS, S., RICHARDS, D., STEVENSON, G.W., 1992. Relation of pyloric motility to pyloric opening and closure in healthy subjects. Gut 33, 466–471. doi:10.1136/gut.33.4.466

XUE, Z., FERRUA, M.J., SINGH, P., 2012. Computational Fluid Dynamics Modeling of Granular Flow in Human Stomach. Aliment. Hoy 21, 3–14.

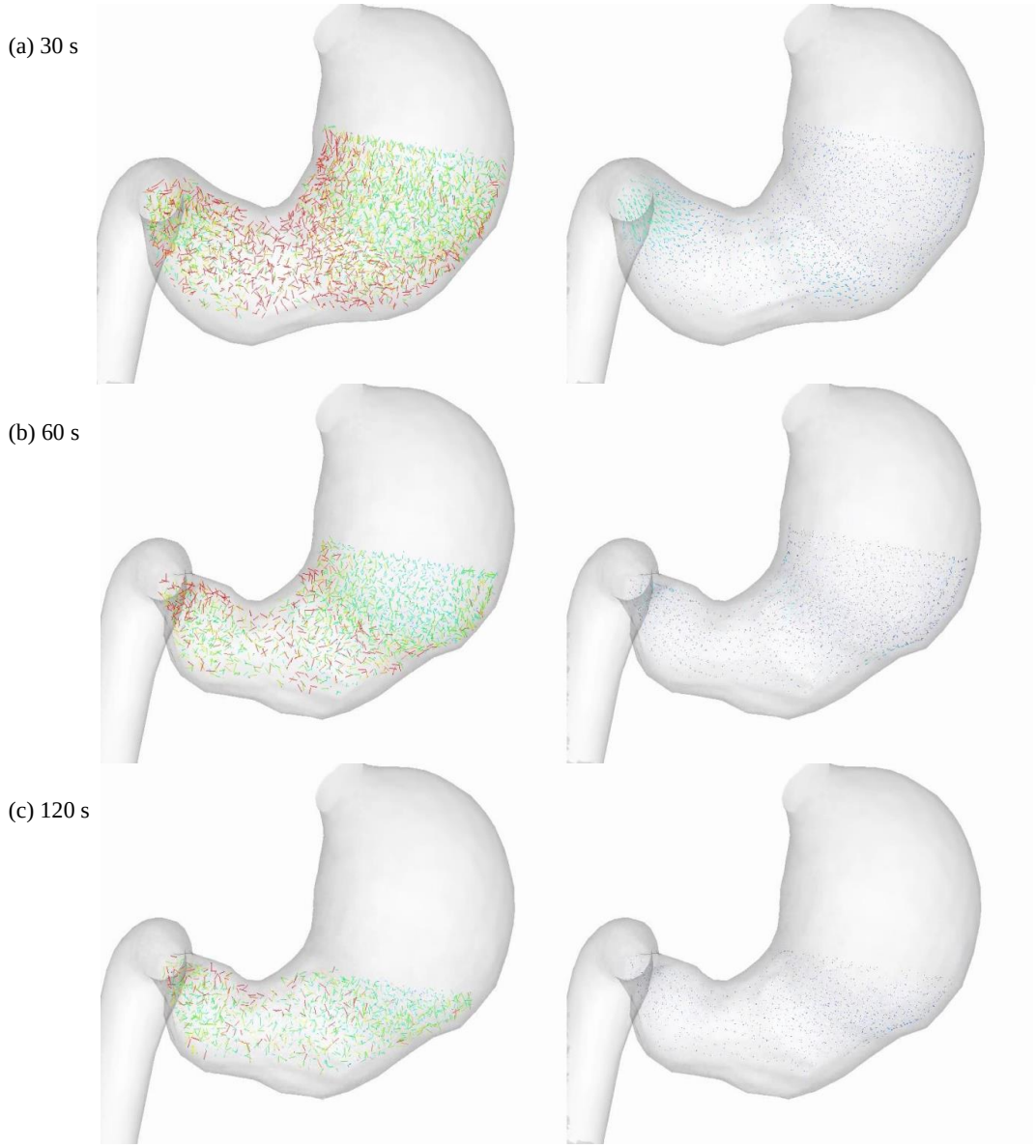

Figure 5: Fluid flow in a cross-section of the stomach for an AWC period of 30 s. The vectors have length and colour depending on the fluid speed. The viscosity is: (left) 0.01 Pa.s; and (right) 1.0 Pa.s.

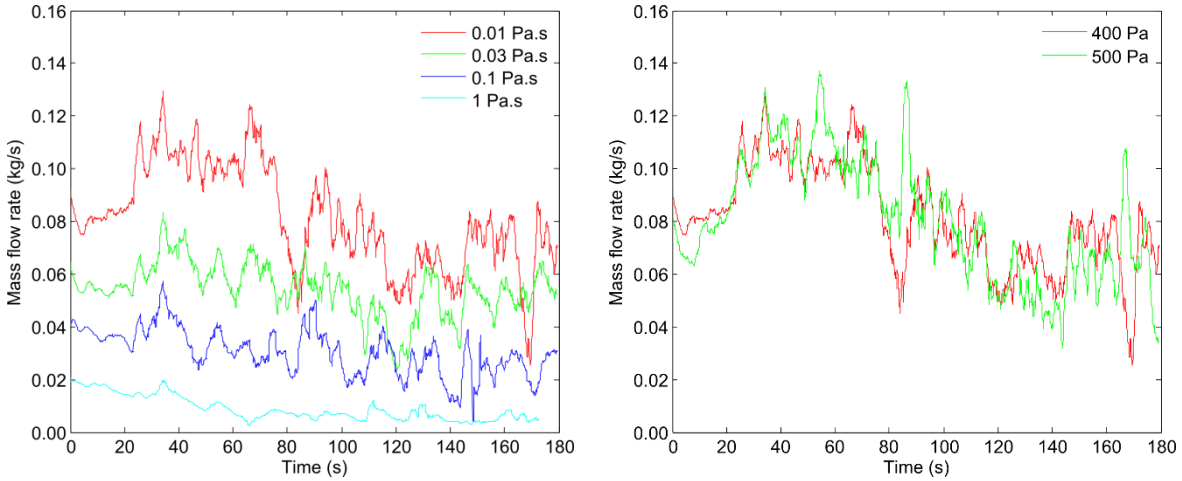

Figure 6: Mass flow rate through the pyloric sphincter for (left) viscosities of 0.01, 0.03, 0.1 and, 1.0 Pa.s, and (right) back pressure conditions of 400 Pa and 500 Pa.